An analysis of global climate variability from homogenously reprocessed GNSS measurements

Ahmed, F. (1), Hunegnaw, A. (1), Teferle, F. N. (1), Bingley, R. (2)

1) Geophysics Laboratory, University of Luxembourg, Luxembourg
2) Nottingham Geospatial Institute, University of Nottingham, United Kingdom

Contact: furqan.ahmed@uni.lu

AGU FM2014 A33A-3148

Abstract

Over the last decade, Global Navigation Satellite Systems (GNSS) have emerged as a precise and cost-effective tool for studying the composition of the atmosphere. GNSS-derived information about tropospheric delay can be used for climate change and variability analysis on a global scale using homogeneously reprocessed GNSS solutions. At the University of Luxembourg, a reprocessed global dataset of GNSS-derived zenith total delay (ZTD) and position estimates, covering 1994-2012, has been produced recently using the Bernese GNSS Software 5.2 (BSW5.2) and the reprocessed products from the Centre for Orbit Determination in Europe. This dataset is based on the network double differencing (DD) strategy. Another experimental dataset covering a shorter period has also been produced using the precise point positioning (PPP) strategy in order to explore its use in climate monitoring. Both of these include over 400 GNSS stations and have been obtained using nearly identical processing settings. The two processing strategies, i.e. DD and PPP, each have their own strengths and weaknesses and could affect the solutions differently at different geographical locations. The aim of this study is to evaluate the quality of the two GNSS-derived tropospheric delay datasets by comparing them to those derived from reanalysis data from the European Centre for Medium-Range Weather Forecasts (ECMWF). Following this, we investigate the inter-annual, seasonal and diurnal climate variability and trends in the tropospheric delay datasets on various regional to global spatial scales.

Introduction

Atmospheric water vapour is the most abundant greenhouse gas and plays a significant role in weather formation, climate change and global warming. Therefore, precise knowledge of the quantity of water vapour in the atmosphere helps in the improvements of weather forecasts and climate monitoring. It is widely known that the propagation delay experienced by GNSS signals, namely the zenith total delay (ZTD), can be converted to integrated water vapour (IWV) using surface meteorological data [1]. As of today, GNSS observations from global networks are available for about the last two decades and this makes it possible to use GNSS as a climate monitoring tool by reprocessing the long-term historical observations and obtaining the IWV trends. Other than its use in climate monitoring, GNSS-derived near real-time ZTD data is assimilated into numerical weather prediction models to improve the short-term weather forecasts. Precise point positioning (PPP) and double differencing (DD) are the common strategies in use today for processing of GNSS observations. PPP solutions are based on single station observations and are mainly affected by the quality of orbit/clock products. DD solutions, on the other hand, are based on differenced observations between the stations in a network and while the dependency on the products is much smaller. DD results are somewhat affected by the distance between stations, especially of remote stations at mid-ocean islands.

In this study, the ZTD dataset obtained by the DD processing strategy has been used to study the variability in climate on different temporal scales for various geographical regions i.e. northern polar, equatorial and southern polar regions. Furthermore, a comparison of DD and PPP ZTD estimates has been conducted in order to study the suitability of the PPP strategy for climate monitoring. The DD and PPP solutions used for this study will hereafter be denoted as DDUL and PPUL, respectively. Table 1 shows the processing characteristics of DDUL and PPUL.

Table 1: Processing characteristics of the ZTD estimation systems

Solution Name:	PPUL	DDUL
Strategy:	PPP	DD
Processing Engine:	BSW5.2 [2]	BSW5.2
ZTD Output Interval:	2 hours	1 hour
Observation Window Used:	24 hours	24 hours
Processing Session Length:	24 hours	24 hours
GNSS Used:	GPS	GPS
A-Priori ZHD Model:	GPT	GPT
Troposphere Mapping Function:	Wet GMF	Wet GMF
Orbit Product Used:	COD Repro1	COD Repro1
Clock Product Used:	COD Repro1	COD Repro1
Antenna Models:	IGS08	IGS08
Coordinates Computed:	Yes	Yes
Elevation Cut-Off Angle:	3°	3°
Ambiguity Resolution:	Yes	Yes

The ground-based GNSS network used in the DDUL solution comprises of around 450 globally distributed stations (Figure 1).

Figure 1 also shows the stations (with names) used to study each of the three regions. The evolution of the number of processed stations with time is shown in Figure 2. The network processed in the PPUL solution is a subset of the DDUL network, which comprises of 76 globally distributed IGb08 core stations from the reference frame network of the International GNSS Service (IGS) [3].

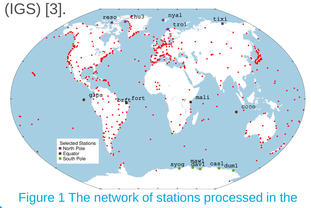

Figure 1 The network of stations processed in the DDUL solution

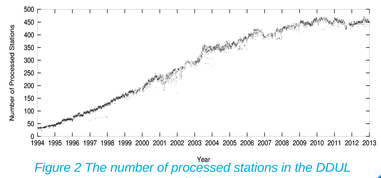

Figure 2 The number of processed stations in the DDUL solution

Acknowledgements
This project is funded by the Fonds National de la Recherche, Luxembourg (Reference No. 1090247). We thank the BIGF, CODE, EUREF and IGS communities for GNSS data and products. The ERA-Interim data was obtained using the TropModel online service of the Geodetic Observatory Pecny.

Presented at: *American Geophysical Union Fall Meeting 2014 | San Francisco | 15-19 December 2014*

Validation of GNSS-Derived ZTD Estimates

Prior to their use in climate monitoring, the GNSS-derived ZTD estimates from the DDUL solution have been validated using the ZTD derived from the European Centre for Medium-range Weather Forecasts (ECMWF)'s reanalysis dataset ECMWF Reanalysis-Interim (ERA-Interim). The ERA-Interim is a global dataset with a grid resolution of 0.75° x 0.75°, temporal resolution of 6 hours, and temporal coverage of 1976 to date (with real-time updates). The ZTD from ERA-Interim at the GNSS station locations has been computed by linear spatial and temporal interpolations from the grid. The validation has been performed by comparing the 3-year long GNSS and ERA-Interim ZTD time series for the selected stations in the three regions.

Figure 3 shows, as an example, the 3-year long time series of GNSS and ERA-Interim ZTD for one IGS station from each region. The stations shown are Ny-Alesund (NYAL) in Svalbard, Cocos (Keeling) Islands (COCO) in Australia, and Syowa (SYOG) in Antarctica.

It can be seen from Figure 3 that the GNSS and ERA-Interim ZTD time series follow the identical pattern for all the three stations. However, there is a millimeter-level bias between the two. The station in the northern polar region (NYAL) has the smallest RMS of the difference whereas the equatorial station (COCO) has the largest RMS. Also, the ZTD has the largest scatter for the equatorial region, which is a consequence of the higher concentration of IWV at the equator.

The RMS differences between the GNSS and ERA-Interim ZTD computed using all the selected stations for every region translate into a difference in IWV of 1.27 kg/m^2 for the northern polar region, 2.62 kg/m^2 for the equatorial region and 1.39 kg/m^2 for southern polar region. The latter is most likely a consequence of the lower sampling in the southern hemisphere.

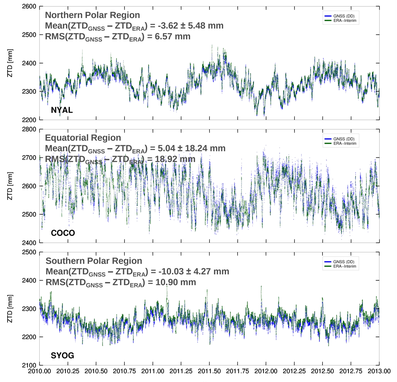

Figure 3 ZTD time series from DDUL solution and ERA-Interim dataset. Notice the different scales of y-axis

Trends and Periodicity in ZTD

In order to study the long-term trend in ZTD at different latitudes, the fully available ZTD estimates from the DDUL solution for the 5 selected GNSS sites in every region have been used. The stations selected to study each of the three regions have at least 70% of data available out of the 19-year period. A linear trend was fitted to the time series (without removing the annual and semi-annual signal) of each of the selected stations and the trends from all the stations for a specific region were averaged. Table 2 shows the values of these averaged trends in ZTD and their equivalent in IWV for each region whereas Figure 4 shows, as an example, the ZTD time series of one station from each region along with fitted linear trends. However, the uncertainties of the computed linear trends are not realistic as they assume randomness and currently do not take into account the stochastic properties of the ZTD time series. Therefore the trend results are preliminary as of now.

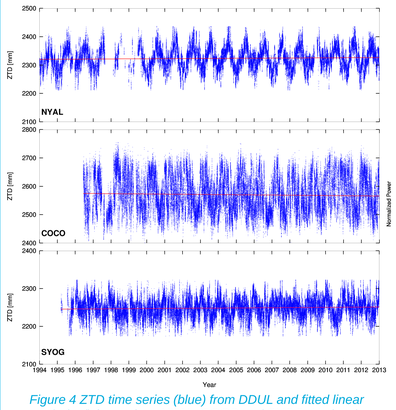

Figure 4 ZTD time series (blue) from DDUL and fitted linear trends (red) for stations NYAL, COCO and SYOG. Notice the different scales of y-axis

Table 2: Mean trends in ZTD and IWV for different regions

Region	ZTD Trend [mm y^{-1}]	IWV Trend [kgm^{-2} y^{-1}]
North Pole	0.20 ± 0.03	0.03 ± 0.001
Equator	0.31 ± 0.07	0.05 ± 0.012
South Pole	0.17 ± 0.02	0.02 ± 0.003

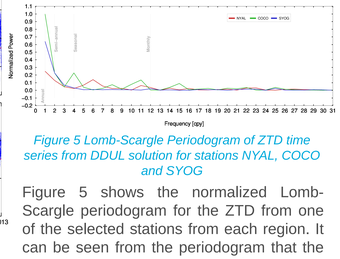

Figure 5 Lomb-Scargle Periodogram of ZTD time series from DDUL solution for stations NYAL, COCO and SYOG

Figure 5 shows the normalized Lomb-Scargle periodogram for the ZTD from one of the selected stations from each region. It can be seen from the periodogram that the annual frequency has the dominant power in all the three cases followed by the semi-annual frequency. Furthermore, the ZTD from the equatorial station COCO also has a seasonal cycle which is not visible in the polar stations.

Inter-Annual and Seasonal Variability in the ZTD

In order to study the inter-annual variability in the ZTD for the northern polar, equatorial and southern polar regions over a decade, monthly means for each individual year from 2003 to 2012 have been computed for a station in each region. Figure 6 shows the station-wise time series of monthly means for each of the ten years along with the mean. It can be seen that the ZTD in the north polar region (NYAL) has the least variation year to year whereas the ZTD inter-annual variation for the equatorial region (COCO) is largest. For the southern polar region (SYOG), the ZTD inter-annual variability is smaller than that in the equatorial region but larger than that observed in the northern polar region.

The seasonal variation in ZTD for the northern polar, southern polar and equatorial regions have been studied by computing the seasonal means for groups of five selected stations in each region. The months of December, January and February are considered as Winter, March, April and May as Spring, June, July and August as Summer and September, October and November as Autumn. Figure 7 shows the time series of seasonal means for each of the three regions. It can be seen that the maximum value of ZTD occurs in Summer for the northern polar region, in Spring for equatorial region and in the Austral Summer for the southern polar region.

Diurnal variation in ZTD (not shown) have also been studied and it is found that its magnitude is highest in the equatorial region and lowest in the northern polar region.

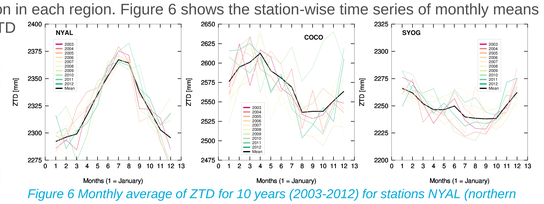

Figure 6 Monthly average of ZTD for 10 years (2003-2012) for stations NYAL (northern polar region), COCO (equatorial region), and SYOG (southern polar region). Note the different scale for every station.

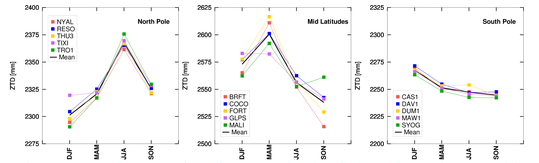

Figure 7 Seasonal average of ZTD for groups of stations in the northern polar, equatorial and southern polar regions. Note the different scale for every region.

Comparison of Precise Point Positioning and Double Differenced ZTD Estimates

The DD processing strategy is generally considered more accurate than the PPP strategy. However, PPP is computationally more efficient than DD network solutions and requires less resources for processing large amounts of data. Therefore, it is of interest to study the suitability of the PPP strategy for climate monitoring applications. To serve this purpose, a comparison of the ZTD estimates from DDUL and PPUL solutions has been conducted for 76 selected IGb08 core stations and the year 2011. The PPUL solution showed a mean bias of 0.01 ± 0.70 mm (≈ 0.002 ± 0.12 kg/m^2 IWV) with an RMS of 0.68 mm (≈ 0.11 kg/m^2 IWV) to the DDUL solution. Figure 8 shows the correlation between the PPUL and DDUL ZTD estimates for the stations NYAL, COCO and SYOG.

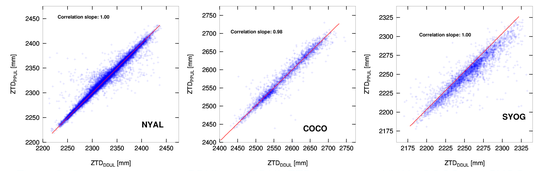

Figure 8: Correlation between PPUL and DDUL ZTD for stations NYAL, COCO and SYOG. Note the different scale for every station.

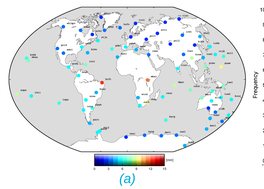

Figure 9: a) Station-wise RMS of the difference between the PPUL and DDUL ZTD b) Histogram of the station-wise mean of the difference between the PPUL and DDUL ZTD along with a normal distribution fit (red).

The histogram of the mean, and the global distribution of the RMS difference between the ZTD from PPUL and DDUL solutions are shown in Figure 9. The variation in PPUL-DDUL bias with latitude is shown in Figure 10, which reports a maximum bias for the equatorial region. The high concentration of column water vapour at the equator is the reason for this latitude dependence of the bias which might reduce by use of the more accurate Vienna mapping function [4].

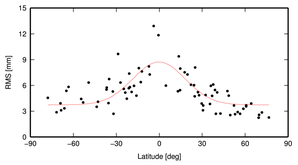

Figure 10: Distribution of the RMS difference (Gaussian fit in red) with respect to latitude between the PPUL ZTD and DDUL ZTD.

Conclusions

A 19-year long global reprocessed GNSS data set based on the double differencing strategy has been used to study the variability of GNSS-derived ZTD on various temporal scales for the equatorial and polar regions. The GNSS-derived ZTD has been validated by comparing it to that derived from the ERA-Interim re-analysis data set for a period of three years. The RMS differences between the GNSS and ERA-Interim ZTD translate to a difference in IWV of 1.27 kg/m^2 for the northern polar region, 2.62 kg/m^2 for the equatorial region, and 1.29 kg/m^2 for the southern polar region.

Linear trends have been obtained for ZTD using the time series for selected stations in the three regions. Positive trends of 0.31 mm y^{-1} (≈ 0.05 kg m^{-2} y^{-1} in IWV), 0.20 mm y^{-1} (≈ 0.03 kg m^{-2} y^{-1} in IWV), and 0.17 mm y^{-1} (≈ 0.02 kg m^{-2} y^{-1} in IWV) were found for equatorial, northern polar and southern polar regions, respectively. Variation in ZTD on inter-annual and seasonal scales have been studied by computing monthly and seasonal averages. It has been found that the maximum value of ZTD occurs in Summer for the northern polar region, in Spring for equatorial region and in the Austral Summer for the southern polar region. Diurnal variation in ZTD have also been studied and it was found that its magnitude is highest in the equatorial region and lowest in the northern polar region.

The ZTD estimates derived from the precise point positioning strategy were compared to those from a double differenced global network solution and an agreement of 0.01 ± 0.70 mm (≈ 0.06 ± 0.12 kg m^{-2} in IWV) has been found between the two. The difference between the ZTD estimated from the two strategies has been found to have a latitude dependence with a maximum around the equator.

References
[1] Bevis, M., S. Businger, Chiswell S., T. A. Herring, R. A. Anthes, C. Rocken, R. H. Ware (1994) GPS Meteorology: Mapping Zenith Wet Delays onto Precipitable Water, Journal of Applied Meteorology, 33(3), 379-386
[2] Dach R (2013) Bernese GNSS Software: New features in version 5.2, Astronomical Institute, University of Bern, Bern, Switzerland
[3] Dow, John M and Neilan, R E and Rizos, C (2009) The International GNSS Service in a changing landscape of Global Navigation Satellite Systems. Journal of Geodesy 83(3-4), 191–198
[4] Boehm J, B Werl, H Schuh (2006a) Troposphere mapping functions for GPS and very long baseline interferometry from European Centre for Medium-Range Weather Forecasts operational analysis data. Journal of Geophysical Research 111 B02406

Scan here to download this poster: